Contents lists available at ScienceDirect

EBioMedicine

Increased expression of yes-associated protein/YAP and transcriptional coactivator with PDZ-binding motif/TAZ activates intestinal fibroblasts to promote intestinal obstruction in Crohn's disease

Weijun Ou[1,#], Weimin Xu[1,#], Fangyuan Liu[1,#], Yuegui Guo[1], Zhenyu Huang[1], Tienan Feng[2], Chen-Ying Liu[1,*], Peng Du[1,*]

[1] Department of Colorectal Surgery, Xinhua Hospital, Shanghai Jiaotong University School of Medicine, Shanghai 200092, China
[2] Clinical Research Institute, Shanghai Jiao Tong University School of Medicine, Shanghai 200025, China

ARTICLE INFO

ABSTRACT

Background: Intestinal obstruction caused by intestinal fibrosis is a common and serious complication of Crohn's disease (CD). Intestinal fibroblasts, the main effector cells mediating gastrointestinal fibrosis, are activated during chronic inflammation. However, the mechanism of fibroblast activation in CD has not been well elucidated.

Methods: Fibroblasts isolated from stenotic and nonstenotic intestines of CD patients were used for RNA sequencing. Immunohistochemical and immunofluorescent staining was performed to evaluate the correlation between intestinal fibrosis and YAP/TAZ expression in our CD cohort and a DSS-induced chronic colitis murine model. A Rho-associated coiled-coil-containing protein kinase 1 (ROCK1) inhibitor was used to explore the ROCK1-YAP/TAZ axis in intestinal fibroblasts in vitro and DSS-induced chronic colitis murine model in vivo.

Findings: The expression of YAP/TAZ was significantly upregulated in stenotic fibroblasts, which was associated with the YAP/TAZ target gene signature. YAP/TAZ knockdown suppressed the activation of intestinal fibroblasts. In intestinal fibroblasts, YAP/TAZ were activated by the Rho-ROCK1 signalling pathway. High YAP/TAZ expression was positively correlated with ROCK1 expression, which is a prognostic marker for intestinal obstruction in CD patients.

Interpretation: YAP/TAZ activation can lead to fibroblast activation and intestinal obstruction in CD. The effect of ROCK1 inhibitor on alleviating intestinal fibrosis is associated with YAP/TAZ inhibition. Targeted inhibition of YAP/TAZ in fibroblasts may be a potential therapeutic strategy to suppress intestinal fibrosis in CD.

Funding: This work was supported by the National Key R&D Program of China (2019YFC1316002), the NSFC (81873547, 82073201, 81874177, 82000481) and the Shanghai Sailing Program (20YF1429400).

Introduction

As a major form of inflammatory bowel disease (IBD), Crohn's disease (CD) is characterized by chronic inflammation and recurrent healing of the mucosa, which results in extracellular matrix (ECM) deposition on the mucosa and submucosa, leading to structural fibrosis and the development of intestinal obstruction.[1] Approximately 30% of CD patients eventually develop end-stage intestinal fibrosis,[2]

and approximately 80% of CD patients eventually undergo fibrotic intestine removal surgery due to intestinal obstruction.[3] However, currently, there are no effective antifibrotic therapies for intestinal fibrosis in CD.[4]

Fibroblasts located in connective tissue around parenchymal cells can produce and secrete collagen, cytokines and other ECM components. Under physiological conditions, the normal structure and physiological function of fibroblasts in the stationary state are necessary to maintain homeostasis of the intestinal microenvironment.[5] Nevertheless, in inflammation, fibroblasts are activated by various signalling pathways, such as TGF-β/SMAD, Wnt/β-catenin, JNK/STAT3, MAPK and Rho-ROCK.[6] Activated fibroblasts differentiate into myofibroblasts with α-smooth muscle actin (α-SMA) expression and induce fibrotic phenotypes with proliferation, matrix deposition, and

* Corresponding author: Peng Du, Department of Colorectal Surgery, Xinhua Hospital, 1665 Kongjiang Road, Shanghai 200092, China; Tel: 086-021-25077858
E-mail addresses: liuchenying@xinhuamed.com.cn (C.-Y. Liu), dupeng@xinhuamed.com.cn (P. Du).
# Weijun Ou, Weimin Xu and Fangyuan Liu contributed equally.

Research in context

Evidence before this study

Intestinal obstruction caused by intestinal fibrosis is the most common complication of Crohn's disease (CD). A small molecule Rho kinase inhibitor (AMA0825) showed an antifibrotic effect in chronic intestinal inflammation-induced fibrosis, but the underlying molecular mechanisms remain obscure.

Added value of this study

Increased expression and activation of Yes-associated protein (YAP) and transcriptional coactivator with PDZ-binding motif (TAZ), transcriptional coactivators and effectors of the Hippo pathway activate intestinal fibroblasts and promote intestinal fibrosis in CD. ROCK inhibition suppresses YAP/TAZ expression and YAP/TAZ-dependent transcription of fibrotic genes.

Implications of all the available evidence

Targeted inhibition of YAP/TAZ in fibroblasts may be a candidate treatment for CD-related intestinal fibrosis to prevent the development of intestinal obstruction.

anti-apoptotic activity, which are regarded as the primary drivers that facilitate organ fibrosis, including intestinal fibrosis.[5] With fibroblast activation, a large amount of collagen is produced and gathered around parenchymal cells, leading to dysregulated microenvironmental homeostasis, excessive fibrosis, abnormal tissue function and even drug resistance.[7] Furthermore, upon fibroblast activation, various chemokines and growth factors are released in the cellular microenvironment, which promotes the inflammatory response, further destroys the structure and function of tissue and aggravates disease. Thus, fibroblast activation is considered to be the main driver promoting fibrotic diseases. Clinically, the development of fibrosis can be postponed by removing harmful stimuli, inhibiting the inflammatory response and promoting matrix degradation. Recently, with the clinical application of cytokine inhibitors and tyrosine kinase inhibitors, these treatments have shown efficacy in lung fibrosis by inhibiting fibroblast activation and profibrotic mediators.[8,9] However, there is a lack of effective therapies for intestinal fibrosis in the clinic. Recurrent inflammation of the intestine in CD triggers tissue repair and regeneration. After excessive repair, myofibroblasts proliferate abnormally, leading to ECM deposition and intestinal stenosis.[10] The mechanism of intestinal fibroblast activation has not been fully elucidated and could provide new therapeutic targets for intestinal fibrosis.

Yes-associated protein (YAP) and transcriptional coactivator with PDZ-binding motif (TAZ) are transcriptional coactivators and effectors of the Hippo signalling pathway.[11] YAP/TAZ activity is negatively regulated by the Hippo pathway. As the Hippo signalling pathway is activated, the phosphorylation cascade with upstream mammalian sterile-20-like kinase 1/2 (MST1/2) and large tumour suppressor kinase 1/2 (LATS1/2) promotes YAP/TAZ phosphorylation, which leads to cytoplasmic retention and protein degradation of YAP/TAZ and inhibits YAP/TAZ transcriptional activity.[12] YAP/TAZ play diverse vital roles in various biological processes, including fibrosis. YAP/TAZ were first found to be required for the generation and function of cancer-associated fibroblasts. Numerous studies have connected YAP/TAZ to fibrosis-related signals.[6,13] By activating mesenchymal cells, YAP/TAZ enhances matrix deposition, metabolic reprogramming metabolism and signal transduction of transforming growth factor-β (TGF-β) and Wnt signalling, which promotes fibrosis in the heart, liver, kidneys, skin, and other organs.[14-16] Expression of YAP/TAZ in pulmonary fibroblasts in patients with idiopathic pulmonary fibrosis promotes the development of pulmonary fibrosis.[17] During chronic liver damage, YAP activation is a key driver of sustained

hepatic stellate cell activation by mediating integrin β1 expression.[18] In vitro, YAP/TAZ knockdown and/or the YAP inhibitor verteporfin depresses the differentiation of hepatic stellate cells and attenuates liver fibrosis. In addition, overexpression of YAP/TAZ in tubular epithelial cells promotes cell proliferation and epithelial-mesenchymal transition (EMT).[19] Molecular mechanism studies have revealed that YAP/TAZ cooperates with the transcription factors AP-1 and Smad7 to regulate TGF-β signal transduction and activate human skin fibroblasts.[14] These studies provide evidence that inhibition of YAP/TAZ can prevent or even reverse fibroblast activation to alleviate the progression of fibrotic diseases in multiple organs.[17] However, the effect of YAP/TAZ on the activation of intestinal fibroblasts and the development of intestinal fibrosis in CD remains unclear.

Rho-associated coiled-coil-containing protein kinase (ROCK) is a serine/threonine kinase involved in several cellular processes, such as cytoskeletal composition, EMT and autophagy, and regulates cell proliferation, differentiation, and migration.[20] ROCK1 mediates the biological function of fibroblasts and plays an important role in pathological inflammation. When RhoA-GTP activates ROCK1, various proteins are phosphorylated, such as myosin light chains, leading to decreased dissociated globular actin, actin gathering and the occurrence of stress fibres.[21,22] ROCK1 is regarded as a potential candidate for antifibrotic therapy.[22] A small molecule ROCK inhibitor showed antifibrotic effects in a chronic intestinal inflammation-induced fibrosis model. Mechanistically, inhibition of ROCK1 induces translocation of myocardin-related transcription factor (MRTF) to the cytoplasm, thus inhibiting gene expression involved in cell differentiation and cytoskeletal composition.[22] YAP/TAZ activation has been found to be related to the Rho/ROCK signalling pathway. As the nucleus relays mechanical signals, YAP/TAZ activity is triggered by ECM stiffness and cell shape, which is regulated by Rho GTPase activity and tension of the actomyosin cytoskeleton.[23] However, whether YAP/TAZ is regulated by Rho/ROCK has not been demonstrated in an experimental colitis-induced intestinal fibrosis model.

In the present study, we report the profibrotic function of YAP/TAZ in CD intestinal fibrosis. YAP/TAZ expression is increased in the stenotic intestines of CD patients and is associated with poor clinical outcomes. We also found that YAP/TAZ promotes intestinal fibrosis by activating intestinal fibroblasts and that the antifibrotic effect of a ROCK1 inhibitor on alleviating intestinal fibrosis was associated with downregulation and inhibition of YAP/TAZ. Therefore, targeting YAP/TAZ in intestinal fibroblasts may be a potentially effective strategy to prevent the development of intestinal fibrosis in CD patients.

Methods

Study population and patient specimens

A retrospective cohort covering 41 eligible CD patients was used in this study. The CD patients were enrolled and followed up from July 2010 to July 2020 at the Department of Colorectal Surgery, Xinhua Hospital, Shanghai Jiao Tong University School of Medicine. CD diagnosis was based on clinical, endoscopic, and histologic criteria. A fibrostenotic intestine was defined according to the Montreal classification,[24] and fibrotic stenosis was confirmed by CT imaging, endoscopy and surgery specimens. The tissue samples used in this study were derived from the small intestine. The area of stenosis was identified by two independent pathologists using macroscopic evaluation and was confirmed by histology.

Inclusion and exclusion criteria

The inclusion criteria were as follows: (1) positive diagnosis of CD; (2) age at diagnosis $\geq$18 years old; and (3) regular follow-up with full clinical data at our department. The exclusion criteria were as follows: (1) patients who were diagnosed with ulcerative colitis (UC),

indeterminate colitis or familial adenomatous polyposis (FAP); (2) poor treatment compliance; and (3) patients with underlying disease or impaired general health and/or patients who were lost to follow-up.

In this study, poor treatment compliance refers to patients who refused to receive regular follow-up and provide feedback to the doctor. Underlying disease was mainly defined as infectious factors caused by intestinal inflammation as well as high-grade dysplasia or colorectal cancer (CRC). Impaired general health refers to chronic and serious diseases leading to poor general conditions, such as diabetes, hypertension, hyperthyroidism or heart failure.[25]

Fibroblast isolation

Human intestinal fibroblasts were derived from CD patients (both stenotic and nonstenotic regions).[26] In brief, intestinal tissues were washed for 30 min at 37°C in medium while shaking and then digested with an enzyme mix containing DNase I (1000 U/mL, Sigma-Aldrich, USA), collagenase (0•1 U/mL, Sigma-Aldrich, USA), and Dispase II (1•5 U/mL, Sigma-Aldrich, USA) until the samples were fully dissolved. Cells were cultivated with FGM^{TM}-2 Fibroblast Growth Medium-2 (Lonza, Basel, Switzerland) supplemented with 1% penicillin/streptomycin.

mRNA sequencing analysis

Total RNA was extracted from primary human intestinal fibroblasts isolated from the stenotic intestines of CD patients using TRIzol reagent according to the manufacturer's instructions. Libraries were then established using a TruSeq Stranded mRNA LTSample Prep Kit (Illumina, San Diego, CA, USA) according to the manufacturer's instructions. Raw data were processed using Trimmomatic software. The reads containing "poly-N" and "low-quality reads" were removed to obtain clean reads. Then, the clean reads were mapped to the reference genome using HISAT2. Differentially expressed genes were identified using the DESeq (2012) R package functions estimateSize-Factors and nbinomTest (The R Foundation, Vienna, Austria). A p-value < 0.05 and fold change > 2 were set as the threshold conditions for significant differential expression. Transcriptome sequencing and analysis were conducted by OE Biotech Co., Ltd. (Shanghai, China).

Small interfering RNA (siRNA) transfection

The siRNAs targeting human YAP and TAZ were as follows: YAP siRNA, GACAUCUUCUGGUCAGAGA and CUGGUCAGAGAUACUUCUU; TAZ siRNA, ACGUUGACUUAGGAACUUU and AGGUACUUCCUCAAU-CACA. The siRNAs and nonspecific control siRNA duplexes were synthesized, desalted, and purified by Shanghai Jima Gene Co., Ltd. (Shanghai, China). Human primary intestinal fibroblasts were seeded at approximately 1×10^5 cells/well one day before sectioning, and then, fibroblasts were transfected with siRNAs in six-well plates using serum-free Opti-Minimal Essential Medium solution (Gibco, USA) with Lipofectamine RNAiMAX (Invitrogen, USA) for 72 h before RNA and protein collection.

Real-time quantitative polymerase chain reaction (RT-qPCR)

Three paired human primary intestinal fibroblast samples were used to detect the expression levels of YAP/TAZ and their downstream target genes. Each case represented an individual CD patient. Cells used in the RT-qPCR experiment were seeded at approximately 2×10^5 cells in a 6 cm dish. Total RNA was extracted from the cultured cells using TRIzol reagent according to the manufacturer's instructions. Reverse transcription was performed with 1 μg of total RNA using PrimeScript^{TM} RT Master Mix (Takara Biomedical Technology Co., Ltd., Beijing, China). qRT-PCR was carried out using SYBR

Premix Ex Taq^{TM} and an Applied Biosystems 7500 Fast Real-Time PCR system (Foster City, CA, USA). Relative mRNA expression was evaluated using the $2^{-\Delta\Delta Ct}$ method and normalized to the expression of GAPDH.[27] All experiments were performed in triplicate. Case 1, Case 2 and Case 3 represent three paired samples from three individual CD patients. The sequences of the PCR primers used in this study are listed in Supplement Table 2.

Immunoblotting

Cells were lysed with 1% NP40 lysis buffer (Sangon Biotech Co., Ltd., Shanghai, China) supplemented with NaF (Sangon Biotech Co., Ltd., Shanghai, China), Na$_3$VO$_4$ (Sangon Biotech Co., Ltd., Shanghai, China), and a protease inhibitor cocktail. Lysates comprising equal amounts of protein were loaded, separated via sodium dodecyl sulfate polyacrylamide gel electrophoresis, and transferred onto a nitrocellulose membrane (Millipore, USA). After blocking with 5% nonfat milk for 1 h, the membrane was incubated with a specific antibody at 4°C overnight. Tris-borate saline with 0.1% Tween-20 was used to wash the membrane. The specific protein was visualized with a horseradish peroxidase (HRP)-conjugated secondary antibody (Beyotime Biotechnology, Shanghai, China) and enhanced chemiluminescence.[28] The antibodies used are listed in Supplementary Table 2.

Mice and the dextran sulfate sodium (DSS)-induced murine colitis model

Six-week-old specific pathogen free (SPF) C57BL/6 male mice (weighing 20 g each) were used to construct a chronic inflammation animal model. All animals were purchased from the Experimental Animal Center of the Chinese Academy of Sciences (Shanghai, China) and maintained in SPF animal experiment room (constant temperature of $20 \pm 3°C$ with $55\% \pm 10\%$ humidity and 12 h light/dark cycle) in Xinhua Hospital, Shanghai Jiaotong University School of Medicine. Chronic inflammation was induced by 2% DSS in 3 cycles of 7 days followed by 2 weeks of tap water.[29] Each mouse was monitored for body weight, activity, and certain conditions, such as diarrhoea and bloody stools, during colitis model building. All mice were euthanized after establishment of the chronic inflammation model and performance of the required experiments. No anaesthetic was used in animal experiments.

DSS-induced chronic colitis murine model treated with ROCK1 inhibitor

Mice were randomly assigned to control and experimental groups (n = 5 each group) according to a computer-generated sequence. Mice were treated with 2% DSS (in total 3 cycles) to induce chronic inflammation and, in the last cycle, were intraperitoneally injected with vehicle or ROCK1 inhibitor (15 mg/kg/day).[30] Nine weeks later, the chronic colitis was established. All surviving mice were sacrificed for subsequent analysis. Mice that died before completion of the 9-week experimental protocol were excluded from further data analysis. Investigators who performed endpoint analyses were blinded to group allocation.

Histopathologic analysis and evaluation of inflammation and fibrosis

For histopathologic evaluation, paraffin-embedded colon sections were stained with haematoxylin−eosin (H&E), Masson's trichrome, or Sirius Red. Histological changes were assessed in both murine and human H&E-stained sections. The inflammation score of the acute and chronic colitis models determined by H&E staining included tissue damage (0=none, 1=isolated and focal epithelial injury, 2=mucosal erosion and ulcers, and 3=extensive damage to the entire intestinal wall) and inflammatory cell infiltration (0=few, 1=increased neutrophils in mucosa, 2=inflammatory cell mass in mucosa and submucosa, and 3=infiltration of inflammatory cells in all layers), as

previously reported.[31] Fibrotic alterations were reflected by the fibrosis score determined from Masson's trichrome staining. The fibrosis score used in patient samples as reported by Zappa et al.[32] included 3 grades: 0=fibrosis limited to the submucosa, 1=massive submucosal fibrosis with preserved layers, and 2= massive transmural fibrosis with effacement of normal layers. Fibrosis in the animal models was quantified using a combined score of fibrosis severity (0=none, 1=increased ECM deposition in the mucosa, 2=increased ECM deposition in the submucosa, 3=thickening of the muscularis mucosae in addition to ECM deposition in the submucosa, 4=thickening of the muscularis propria in addition to ECM deposition in the submucosa, and 5=ECM deposition in the serosa layers) and circularity (1=0-25%, 2=25-50%, 3=50-75%, and 4=75-100%).[33] The data were analysed in a blinded manner and confirmed by an independent second observer.

Immunofluorescence (IF) staining of cultured cells

Cells grown on cover slides were fixed with 4% paraformaldehyde for 30 min and then permeabilized by exposure to 0.1% Triton X-100 for 10 min. After blocking in 3% bovine serum albumin (BSA) for 30 min at room temperature, the cells were incubated with primary antibodies (1:100 anti-α-SMA and 1:100 anti-YAP) in 1% BSA for 2 h at room temperature. After washing with phosphate-buffered saline (PBS), the cells were incubated with Alexa Fluor 594-conjugated goat anti-rabbit IgG and Alexa Fluor 488-conjugated goat anti-mouse IgG in the dark for 1 h. Finally, the cells were counterstained with 5 μg/mL 4′,6-diamidino-2-phenylindole and analysed using fluorescence microscopy (OLYMPUS, Japan).

Immunohistochemistry (IHC) and IF

Paraffin-embedded tissues were deparaffinized in xylene and rehydrated with descending concentrations of ethanol. Antigen was retrieved in citrate buffer by heating, and nonspecific binding was blocked with 3% hydrogen peroxide (Sangon Biotech Co., Ltd., Shanghai, China) and 5% goat serum (Beyotime Biotechnology, Shanghai, China). The slides were then incubated with specific antibodies at 4°C overnight. After thorough washing with PBS three times, the slides were incubated with an HRP-labelled secondary antibody for 1 h. Diaminobenzidine chromogen was used for the chromogenic reaction. For IF staining, Alexa Fluor 488-conjugated anti-mouse IgG and SABC Cy3-conjugated anti-rabbit IgG were used as secondary antibodies.

The YAP/TAZ and α-SMA positive cells in the intestinal stroma were counted under microscope. The stroma was defined as the population of stromal cells surrounding the identifiable intestinal crypt but did not include identifiable blood/lymphatic vessels or muscular tissue. Ten samples in total were evaluated by immunofluorescence staining. Quantifications were performed with the average values in 3 representative high-power fields per sample. The average number of YAP/TAZ⁺ stromal cells in every sample was used to analyse the correlation with the number of α-SMA⁺ cells.

Histopathologic evaluation of YAP/TAZ and ROCK1 expression levels

The YAP/TAZ and ROCK1 expression levels in the intestinal tissues of CD patients were evaluated and semiquantitatively scored by two independent pathologists based on the IHC results. The final scores for each CD patient were calculated by multiplying the proportion score and the intensity score. The detailed scoring methods were based on previous research.[34] The staining proportion criteria were as follows: 0=0%, 1=0-25%, 2= 25-50%, 3=50-75%, and 4=75-100%. The staining intensity was scored from 0 to 3. In this study, clinical patient samples with a staining score $\leq$ 6 were considered to exhibit low expression, and those with a score > 6 were regarded as having high expression. This method was also used for IHC analysis of YAP/TAZ expression in the chronic colitis model.

Cell counting kit-8 (CCK-8) experiment

The CCK-8 assay was employed to detect the effect of YAP/TAZ knockdown on cell proliferation. First, 500 cells/well were seeded and cultured with FGM™-2 Fibroblast Growth Medium-2 in 96−well plates, with five replicates for each siRNA transfection group. After incubation for 24 h, 10 μl/well CCK−8 solution was added to each well in the first 96−well plate and incubated with the cells for 1.5 h at 37°C in dark conditions. A microplate reader was used to detect the absorbance at 450 nm in each plate at 1, 3 and 5 days.

Ethical statements

The clinical study was approved by the Ethics Committee of Xinhua Hospital (No. XHEC-D-2020-147). All patients signed an informed consent form prior to the study. The protocol for animal experiments was carried out in accordance with institutional animal welfare guidelines and followed the ARRIVE guidelines for reporting animal research. An ARRIVE guideline checklist is included in Supplementary Checklist 1. All animal experimental procedures were approved by the Laboratory Animal Care and Welfare Committee of Xinhua Hospital (No. XHEC-F-2020-021).

Statistical analysis

GraphPad Prism 8 software (GraphPad Software, San Diego, CA, USA) and SPSS Statistics 25 software (IBM SPSS Statistics, Chicago, IL, USA) were used for statistical analyses. Data are expressed as means $\pm$ standard deviation (S.D). The Kaplan-Meier method was used to assess the survival time distribution, and a log-rank test was used to test for significance in intestinal obstruction-free survival among the different prognostic groups. Receiver operating characteristic (ROC) curve analysis was used to determine the best YAP/TAZ and ROCK1 cut-off values for predicting the occurrence of obstruction. The Kaplan−Meier method with a log-rank test was performed to further demonstrate intestinal obstruction-free survival with different values of YAP/TAZ and ROCK1. Multivariate logistic regression was performed to analyse the factors associated with intestinal obstruction. Odds ratios (ORs) and 95% confidence intervals (CIs) for multivariate analysis were calculated using the logistic regression model. Student's t test was used to compare differences between two groups. Data that were not normally distributed were analysed using a Mann-Whitney U test. Pearson's correlation test was performed to analyse the relationship between the expression of YAP and α-SMA in CD patient samples. Spearman's correlation test was used to determine the relationship between the YAP/TAZ score and the ROCK1 score. All statistical tests were two-sided, and a p-value of < 0•05 was considered statistically significant.

Results

YAP/TAZ expression is increased in stenotic intestines and associated with poor clinical outcomes in CD

A retrospective cohort covering 41 eligible CD patients was used in this study, with a median follow-up time of 48 months (24-120)

Table 1
Main baseline characteristics of patients

Variables	All case (n=41)
Sex(male/female)	22/19
Age at diagnosis, n (%)	
A1	3 (7.3)
A2	22 (53.7)
A3	16 (39.0)
Follow-up time [month, median (IQR)]	48 (24.0-120.0)
CDAI [score, median (IQR)]	115.24 (90.15-148.74)
Extraintestinal manifestations (EIMs), n (%)	11 (26.8)
Family history, n (%)	
No	39 (95.1)
Family history of CRC or IBD	0 (0)
Family history of other autoimmune disease	2 (4.9)
History of surgery, n (%)	23 (56.1)
Location of CD, n (%)	
L1	21 (51.2)
L2	7 (17.1)
L3	11 (26.8)
L4	2 (4.9)
Behavior of CD, n (%)	
B1	5 (12.2)
B2	27 (65.9)
B3	9 (22.0)
Mesalamine, n (%)	27 (65.9)
Biologics, n (%)	11 (26.8)
Steroids, n (%)	13 (31.7)
Immunomodulators, n (%)	14 (34.1)
Hb (g/L, mean ± SD)	115.34±18.33
Alb (g/L, mean ± SD)	35.21±5.64

Age of diagnosis was divided into A1, A2 and A3 according to the Montreal classification. A1: before the age of 16; A2: age of 17 to 40; A3: over the age of 40.

IQR, Interquartile range; CRC, Colorectal cancer; IBD, Inflammatory bowel disease; Hb, hemoglobin; Alb, Albumin.

from July 2010 to July 2020. The detailed demographic, clinical, and laboratory characteristics are shown in Table 1, and the normal distribution test of continuous clinical variables is shown in Supplementary Table 1.

IHC staining was performed to assess the expression of YAP/TAZ in the lesion sites of 41 CD patients and in adjacent normal intestinal tissues. Representative images of the differential expression of YAP/TAZ are shown in Figure 1a and d, including negative, weakly positive, moderately positive, and strongly positive YAP/TAZ expression. We also observed that the IHC signals of YAP/TAZ mainly accumulated in the nucleus in the YAP/TAZ high expression samples, which represents YAP/TAZ activation. The IHC score of YAP had the most significant area under the ROC curve (AUC) of 0•725, with a sensitivity of 78•3% and specificity of 66•7% at a cut-off value of 6 (p = 0•015). A TAZ score of 6 had the largest AUC of 0•653, with a sensitivity of 69•6% and specificity of 61•1% (p = 0•095) (Figure 1b and e). The cohort was divided into YAP/TAZ high expression and low expression groups according to the above cut-off values. Based on this criterion, 24 (58•5%) and 17 (41•5%) samples were categorized into high and low YAP expression groups, respectively. Twenty-three (56•1%) and 18 (43•9%) samples were divided into high and low TAZ expression groups, respectively.

In univariate analysis, the YAP/TAZ expression level was significantly associated with the incidence of intestinal obstruction (YAP: p=0•004; TAZ: p=0•05). YAP expression was associated with CD intestinal obstruction in the multivariate logistic regression analysis (OR=6•796, 95% CI=1•539-30•011, p=0•011) (Table 2). Moreover, Kaplan-Meier survival analysis with a log-rank test demonstrated that CD patients with only high YAP expression had lower intestinal obstruction-free survival (p=0•0464) than those with only low YAP expression (Figure 1c), which indicated that these patients had worse clinical outcomes. Similar results were shown among CD patients with only high TAZ expression (p=0•024) (Figure 1d) and with coexpression of YAP/TAZ (p=0•0310) (Figure 1g). Taken together, these data indicate that stromal YAP/TAZ was upregulated in obstruction tissues and was significantly associated with a worse prognosis in CD patients.

YAP/TAZ downstream target gene signature is enhanced in intestinal fibroblasts from stenotic intestines in CD

To explore the profibrotic mechanisms of intestinal fibroblasts in intestinal obstruction, we performed RNA sequencing of primary human intestinal fibroblasts derived from intestinal stenotic and paired nonstenotic tissues from CD patients. The characteristics of intestinal tissues with and without stenosis are shown in Supplementary Figure 1. Primary intestinal fibroblasts were confirmed by immunofluorescence of fibroblast markers, such as CK18 (-), vimentin (+) and α-SMA (+), using HCT116 epithelial cells as a negative control (Supplementary Figure 2a). RNA sequencing showed that 1109 genes were significantly upregulated and 1020 genes were downregulated in intestinal fibroblasts derived from stenotic tissues compared with those derived from nonstenotic tissues (corrected p-value < 0.05, fold change>2) (Figure 2a). Gene Ontology (GO) analysis suggested that differentially expressed genes were enriched in TGF-β signalling, extracellular matrix organization, and collagen and/or actin binding, which are correlated with the features of fibroblast activation (Figure 2b-d). Interestingly, Gene Signature Enrichment Analysis (GSEA) revealed that the YAP/TAZ downstream target gene signature was enriched in fibroblasts from the stenotic intestine of CD patients (Figure 2e). Thus, these results indicate that YAP/TAZ transcriptional activity is enhanced in intestinal fibroblasts during the progression of intestinal stenosis, which might be correlated with profibrotic activation of intestinal fibroblasts.

YAP/TAZ expression is increased in α-SMA$^+$ fibroblasts in the fibrostenotic intestine

To explore the activation mechanism of YAP/TAZ activity in intestinal fibroblasts, we first examined the expression of YAP/TAZ in fibroblasts derived from stenotic and nonstenotic intestines via RT-qPCR. A significant increase in YAP/TAZ mRNA levels was observed in fibroblasts from stenotic intestines, along with upregulation of the classic target genes, including ANKRD1, CTGF, and CYR61 (Figure 3a). Interestingly, when we compared the expression levels of YAP/TAZ and ANKRD1 in fibroblasts with the expression levels in HCT116 cells, we found that the expression levels of YAP/TAZ and ANKRD1 in fibroblasts were much higher than in epithelial HCT116 cells, which indicated high activation of YAP/TAZ in fibroblasts, especially in stenotic fibroblasts (Supplementary Figure 2b). The increased YAP/TAZ level in stenotic intestinal tissue was confirmed by IHC (Figure 3b-c). We further confirmed the increased YAP/TAZ protein expression in fibroblasts through coimmunofluorescence of YAP/TAZ and PDGFRα (Supplementary Figure 3a-b). Moreover, the protein levels of YAP/TAZ were also increased in fibroblasts expressing α-SMA (Figure 3d-e). Next, we analysed the correlation between YAP and α-SMA in fibroblasts. We observed that the expression of α-SMA was also significantly increased in stenotic intestine tissue, and its level was positively correlated with YAP expression in the stenotic intestines (Pearson correlation coefficient R=0•9140, p < 0•0001) (Figure 3f-i) and with the correlation between α-SMA$^+$ cells and TAZ$^+$ cells (Pearson correlation coefficient R=0•7042, p = 0•0005) (Figure 3j-m). Consistently, in primary fibroblasts cultured in vitro, we observed significantly enhanced YAP/TAZ nuclear localization in fibroblasts derived from stenotic intestines (Figure 3n-o). Altogether, these results indicate that YAP/TAZ is highly expressed and activated in stenotic intestines and derived intestinal fibroblasts, which may play a role in the activation of intestinal fibroblasts.
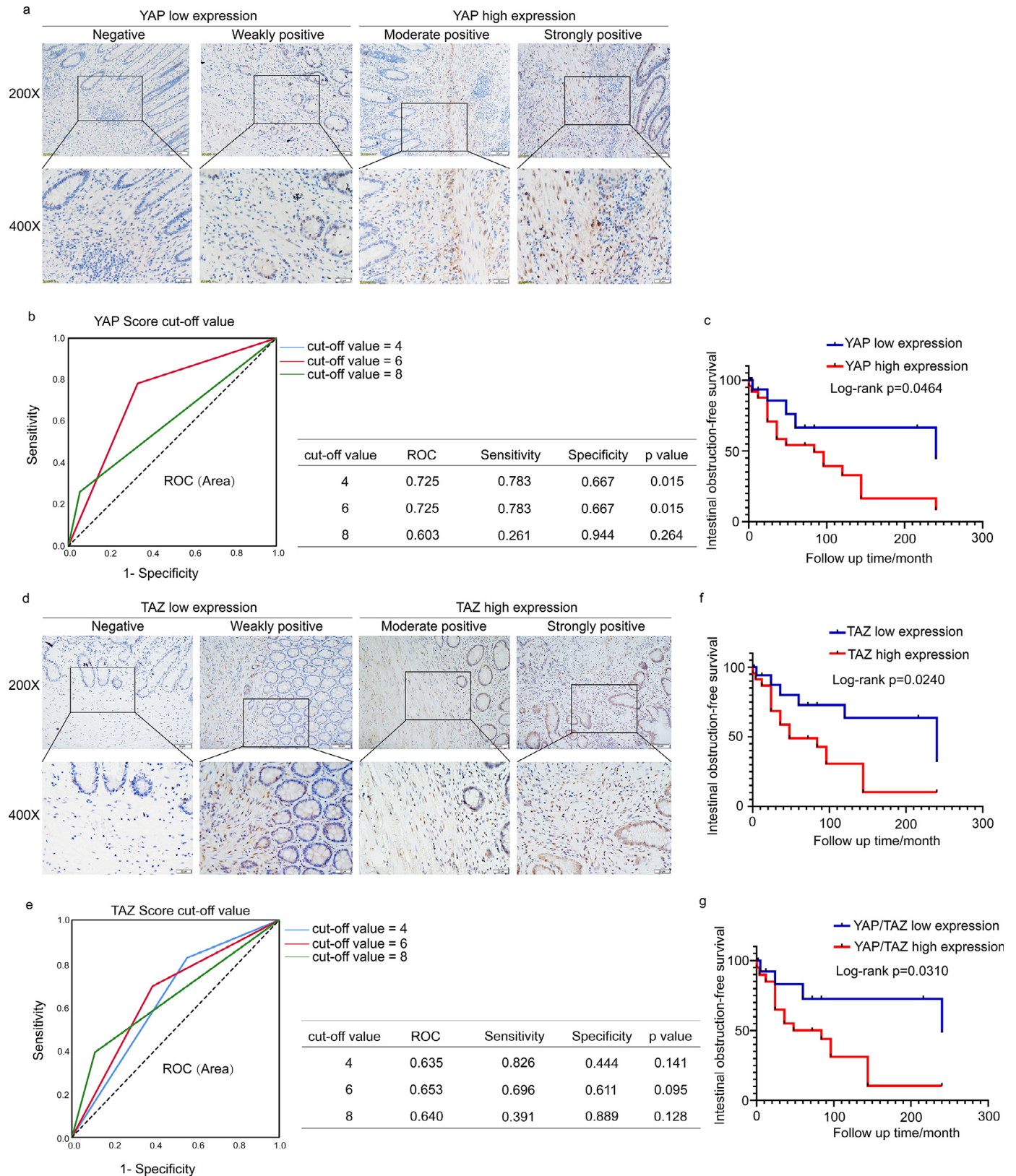
Figure 1. YAP/TAZ expression is increased in stenotic intestines and associated with poor clinical outcomes in CD. (a) Immunohistochemical analysis of different YAP expression levels in CD patients. Scale bar = 50 μm (upper panels) and 20 μm (lower panels). (b) Cut-off value of the YAP expression score in IHC analysis based on the ROC curve. ROC curves of cut-off value=4 and 6 coincide. The sensitivity and specificity of the selected cut-off value are shown in the table near the ROC curve. (c) Kaplan-Meier plots were stratified by YAP expression for intestinal obstruction-free survival in CD patients. (d) Immunohistochemical analysis of TAZ expression in CD patients. Scale bar = 50 μm (upper panels) and 20 μm (lower panels). (e) Cut-off value of the TAZ expression score in IHC analysis based on the ROC curve. (f) Kaplan-Meier plots were stratified by TAZ expression for intestinal obstruction-free survival in CD patients. (g) Kaplan-Meier plots were stratified by YAP/TAZ coexpression for intestinal obstruction-free survival in CD patients. The ROC curve was used to determine the cut-off value. A log-rank test was performed for prognosis analysis. Significant differences are shown by p = <0.05.

Table 2
Univariable analysis of risk factors for stenosis in CD

Variables	Non-obstruction group	obstruction group	Univariate p value	Multivariate Odds Ratio	95% CI	p value
Sex,n(%)			0.295 [a]			
Male	8(36.4)	14(63.6)				
Female	10(52.6)	9(47.4)				
Age at diagnosis, n (%)			0.181 [a]			
A1	0(0.0)	3(100.0)				
A2	9(40.9)	13(59.1)				
A3	9(56.3)	7(43.7)				
Disease duration, n (%)			0.843 [a]			
<10y	12(42.9)	16(57.1)				
≥10y	6(46.2)	7(53.8)				
EIM, n(%)			0.634 [a]			
No	12(40.0)	18(60.0)				
Yes	6(54.5)	5(45.5)				
Family history, n (%)			0.456 [b]			
No	17(43.6)	22(56.4)				
Family history of CRC or IBD	0(0.0)	0(0.0)				
Family history of other autoimmune disease	1(50.0)	1(50.0)				
History of surgery, n (%)			0.567 [a]			
No	7(38.9)	11(61.1)				
Yes	11(47.8)	12(52.2)				
Location of CD, n (%)			0.414 [a]			
L1	10(47.6)	11(52.4)				
L2	2(28.6)	5(71.4)				
L3	6(54.5)	5(45.5)				
L4	0(0.0)	2(100.0)				
Mesalamine, n (%)			0.923 [a]			
No	6(42.9)	8(57.1)				
Yes	12(44.4)	15(55.6)				
Steroids, n (%)			0.632 [a]			
No	13(46.4)	15(53.6)				
Yes	5(38.5)	8(61.5)				
Immunomodulators, n (%)			0.447 [a]			
No	13(48.1)	14(51.9)				
Yes	5(35.7)	9(64.3)				
Biologics, n (%)			0.815 [a]			
No	14(46.7)	16(53.3)				
Yes	4(36.4)	7(63.6)				
Hb, n (%)			0.702 [a]			
≥90g/L	17(44.7)	21(55.3)				
<90g/L	1(33.3)	2(66.7)				
Alb, n (%)			0.397 [a]			
≥35g/L	11(50.0)	11(50.0)				
<35g/L	7(36.8)	12(63.2)				
Expression of YAP, n (%)			0.004 [a]	6.796	(1.539-30.011)	0.011
High expression	6(25.0)	18(75.0)				
Low expression	12(70.6)	5(29.4)				
Expression of TAZ, n (%)			0.050 [a]	3.244	(0.777-13.549)	0.107
High expression	7(30.4)	16 (69.6)				
Low expression	11 (61.1)	7 (38.9)				
Expresion of ROCK1, n (%)			0.004 [a]	5.588	(1.308-23.879)	0.020
High expression	6(25.0)	18(75.0)				
Low expression	12(70.6)	5(29.4)				

[a], Chi-squared; [b], Fisher's exact test; CI, Confidence interval; CRC, Colorectal cancer; IBD, Inflammatory bowel disease; Hb, hemoglobin; Alb, Albumin. EIM: Extra-intestinal manifestation.

YAP/TAZ promotes the expression of profibrotic genes in intestinal fibroblasts

To examine whether YAP/TAZ can affect the expression of profibrotic genes, cultured primary fibroblasts isolated from the fibrostenotic intestines were transfected with YAP/TAZ siRNA. Knockdown of YAP/TAZ was confirmed by qPCR and Western blot analysis (Figure 4a and b). The classic target genes of YAP/TAZ, including *ANKRD1, CTGF*, and *CYR61*, were significantly downregulated by YAP/TAZ knockdown, as were the mRNA levels of the profibrotic genes *ACTA2* and *COL1A1*. Western blotting and IF staining further showed that the expression of α-SMA was downregulated upon YAP/TAZ knockdown (Figure 4b-c). Furthermore, CCK-8 assays revealed decreased cell proliferation of CD-derived intestinal fibroblasts after knockdown of YAP/TAZ (Figure 4d). These data demonstrate that YAP/TAZ can enhance the activation of intestinal fibroblasts by prompting the expression of profibrotic genes and promoting cell proliferation.

ROCK inhibition interferes with the YAP/TAZ-dependent transcriptional activation of fibrotic genes

ROCK is considered a potential target for fibrotic disease treatment.[22] Consistently, GO analysis revealed positive regulation of Rho protein signal transduction in fibroblasts derived from stenotic intestines (Figure 2b and d). Since Rho-ROCK1 signalling has been connected with the activation of YAP/TAZ, we explored whether the Rho/ROCK signalling pathway promotes intestinal fibrosis via YAP/TAZ-dependent transcriptional regulation. We first explored the expression of ROCK1 in fibroblasts derived from stenotic intestines. IHC assays showed that ROCK1 expression was higher in stenotic intestinal tissues (Figure 5a),
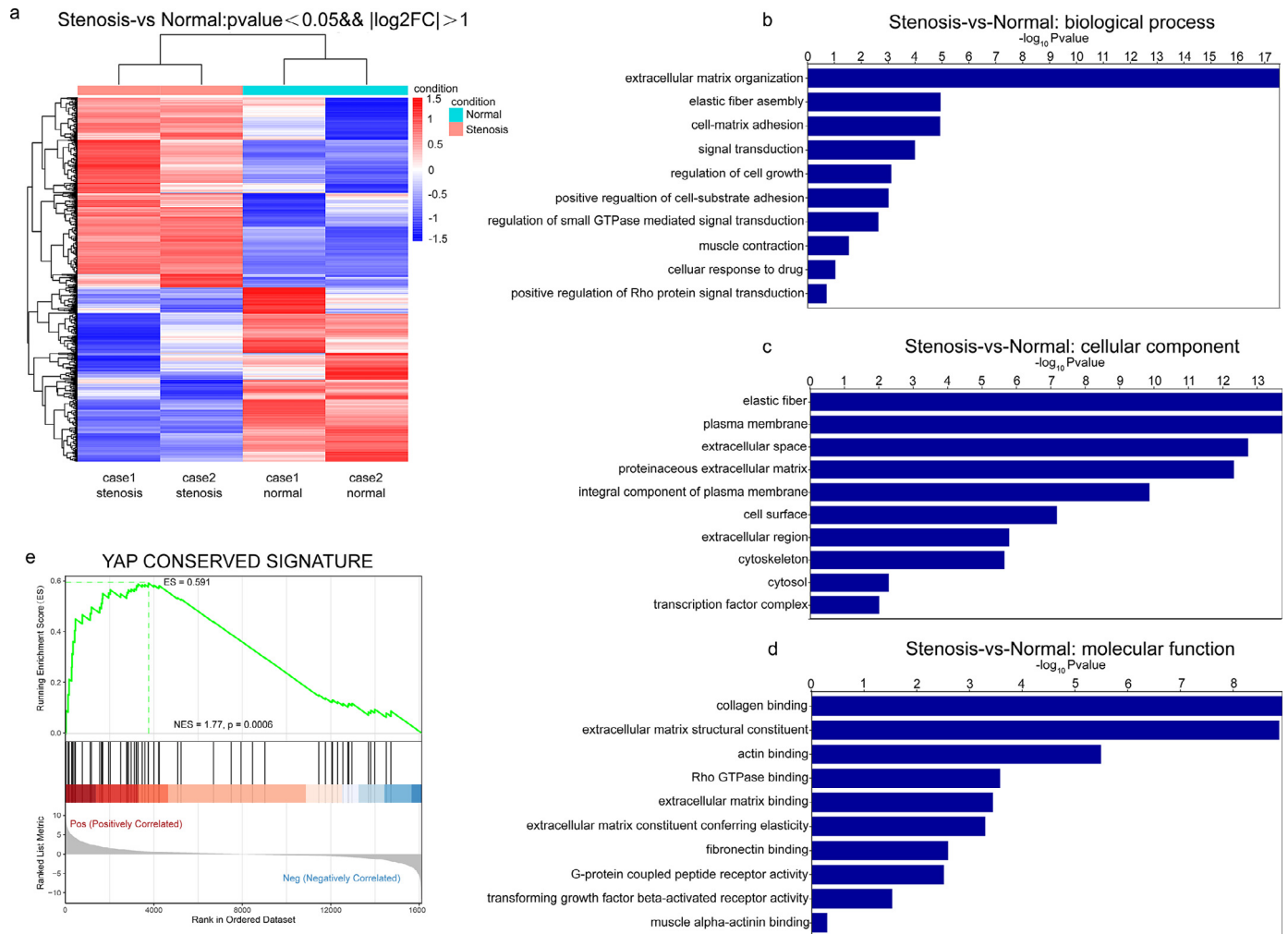
Figure 2. YAP/TAZ is activated in profibrotic intestinal fibroblasts. (a) Primary human intestinal fibroblasts were isolated from stenotic and nonstenotic areas of intestines from CD patients. RNA sequencing and differential expression analysis were performed (corrected p value <0.05, fold change >2). (b-d) GO analysis was used to evaluate differentially expressed genes for biological process, cellular component and molecular function. (e) GSEA indicated enrichment of transcription targets of the YAP conserved signature in fibroblasts from the stenotic intestine of CD patients.

which was consistent with previous studies.[22] In fibroblasts derived from the stenotic intestines of CD patients, Western blot analysis further showed that the ROCK1 protein level was moderately increased compared with that in paired nonstenotic intestines distal to the stenosis from three CD patients (Figure 5b). Then, using RT-qPCR, we examined the YAP/TAZ target genes and fibrotic genes in fibroblasts isolated from stenotic intestines treated with the ROCK inhibitor Y27632. We observed that the mRNA expression levels of *ANKRD1, CTGF*, and *CYR61* were inhibited by Y27632 and that *ACTA2* was also significantly decreased upon ROCK1 inhibition (Figure 5c). Activated LATS1/2 phosphorylates YAP/TAZ, which promotes YAP/TAZ cytoplasmic retention and protein degradation.[35] We observed that Y27632 decreased the protein level of α-SMA, which was correlated with downregulated YAP/TAZ protein levels and increased YAP phosphorylation at Ser127 (Figure 5d). Consistently, Y27632 treatment significantly inhibited YAP/TAZ nuclear localization (Figure 5e-f). Overall, these results suggest that the ROCK inhibitor suppressed the activation of intestinal fibroblasts by inhibiting YAP/TAZ.

Suppression of YAP/TAZ via ROCK1 inhibition in a chronic colitis murine model

To explore whether the ROCK1 inhibitor suppresses YAP/TAZ in fibroblasts in vivo, we established a chronic colitis murine model in which mice were fed drinking water containing 2% DSS in three cycles (Supplementary Figure 4a). These mice developed chronic intestinal inflammation and fibrosis that manifested as a shortened colon and more severe colonic tissue damage, inflammatory cell infiltration, and collagen deposition than control mice (Supplementary Figure 4b-c). Similar to the findings in CD intestinal tissues, YAP/TAZ expression was significantly increased in inflamed intestines from DSS-fed mice, as evidenced by IHC staining (Supplementary Figure 4d-e).

Next, we explored whether ROCK inhibition decreased YAP/TAZ expression and alleviated intestinal fibrosis in this chronic experimental colitis model. The mice were treated with Y27632 before the third cycle of DSS induction (Figure 6a). Chronic colitis mice treated with the ROCK inhibitor showed less severe manifestations than those in the control group, which was indicated by the length of the colon (Figure 6b). Moreover, H&E staining and Masson's trichrome staining revealed that colon tissues from Y27632-treated mice had a decreased pathological score compared to that in DSS-treated mice (Figure 6c-d). Consistently, IHC analysis showed that the colon tissues from mice receiving Y27632 showed reduced YAP/TAZ expression (Figure 7e-f). IF staining of α-SMA also showed a reduced number of α-SMA+ cells in colonic tissues upon treatment with Y27632 (Figure 7g). ECM deposition plays a critical role in the development of intestinal fibrosis, as assessed by the expression of collagen I and
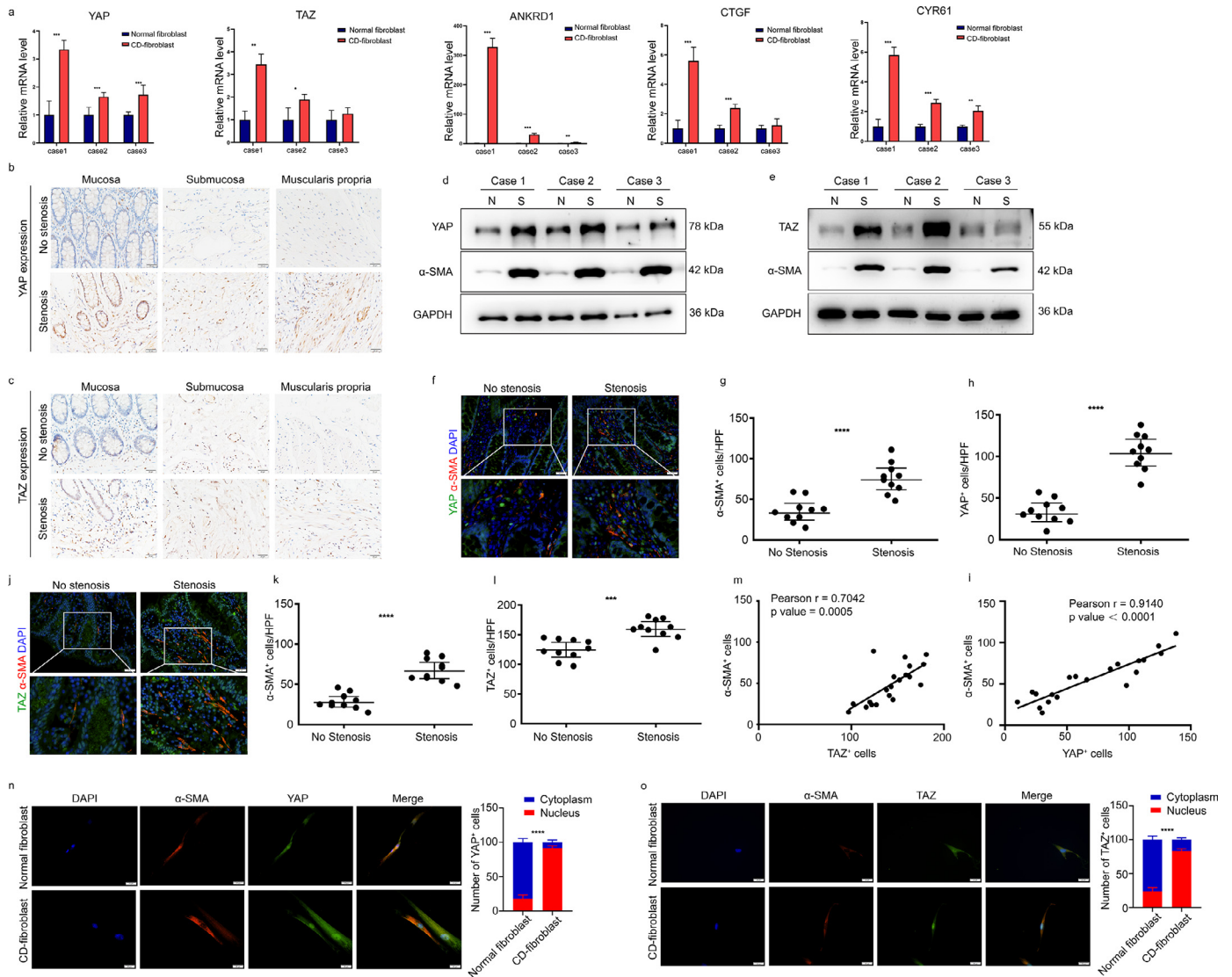
Figure 3. YAP/TAZ expression is increased and correlated with more α-SMA+ cells in CD with fibrostenosis. (a) YAP/TAZ expression was detected in fibroblasts isolated from stenotic and nonstenotic areas of intestines from CD patients via real-time quantitative polymerase chain reaction. (b-c) Representative images of immunohistochemical staining showing the expression of YAP/TAZ in different layers of stenotic and nonstenotic intestinal tissue from CD patients (n=10). Scale bar = 20 μm. (d-e) Western blot analysis of YAP/TAZ expression in 3 paired samples of fibroblasts derived from CD patients with and without stenosis. (f) Intestinal tissues from CD patients with and without stenosis (n=10) were double-stained for YAP and α-SMA, and (g) YAP+ cells and (h) α-SMA+ cells were quantified. Quantifications were performed with the average values in 3 representative HPFs/sample. Scale bar = 20 μm (upper panels) and 10 μm (lower panels). (i) The number of YAP+ cells was evaluated by immunofluorescence staining and correlated with the number of α-SMA+ cells in CD patients with and without stenosis (n=10). (j) Intestinal tissues from CD patients with and without stenosis (n=10) were double-stained for TAZ and α-SMA, and (k) α-SMA+ cells and (l) TAZ+ cells were quantified. Quantifications were performed with the average values in 5 representative HPFs/sample. Scale bar = 20 μm (upper panels) and 10 μm (lower panels). (m) The number of TAZ+ cells was evaluated and correlated with the number of α-SMA+ cells in CD patients with and without stenosis (n=10). (n-o) Representative images of immunofluorescence staining showing the nuclear localization of YAP/TAZ in fibroblasts isolated from stenotic regions. Scale bar = 20 μm. In all cases, the bars in the graphs represent mean ± S.D. Statistical analyses were performed using Student's t test for (a) paired and (d-h, k-l) unpaired samples, Pearson's correlation for (i, m) correlation analysis and a chi-square test for (n-o) cell quantification. Significant differences are shown by *p<0.05, **p<0.01, ***p<0.001, and ****p<0.0001. CD, Crohn's disease; HPF, high-power field; Case 1, Case 2 and Case 3 represent three paired samples from three individual CD patients.

fibronectin (FN1). As shown in Figure 7h and i, treatment with the ROCK inhibitor significantly reduced collagen I and FN1 expression. Altogether, these data indicate that the antifibrotic effect of a ROCK inhibitor in a chronic colitis murine model is associated with reduced YAP/TAZ expression, which suggests that ROCK inhibition may prevent intestinal fibrosis by downregulating YAP/TAZ.

ROCK1 expression is upregulated in CD with intestinal obstruction and correlated with YAP/TAZ expression

Next, we used IHC to assess the correlation between ROCK1 expression and the incidence of intestinal obstruction in our retrospective CD cohort. A representative image of the differential ROCK1 expression is shown in Figure 7a. Twenty-four (58•5%) and 17 (41•5%) samples were categorized into ROCK1 high and low expression groups, respectively, based on the cut-off value determined by the ROC curve (Figure 7b).

In univariate analysis, ROCK1 expression was significantly correlated with the incidence of intestinal obstruction (p=0•004), as reported in previous studies.[22] Additionally, multivariate logistic regression analysis confirmed the correlation between ROCK1 expression and intestinal obstruction in CD (OR=5•588, 95% CI=1•308-23.879, p=0•020) (Table 2). Furthermore, Kaplan-Meier analysis with a log-rank test indicated that patients with high ROCK1
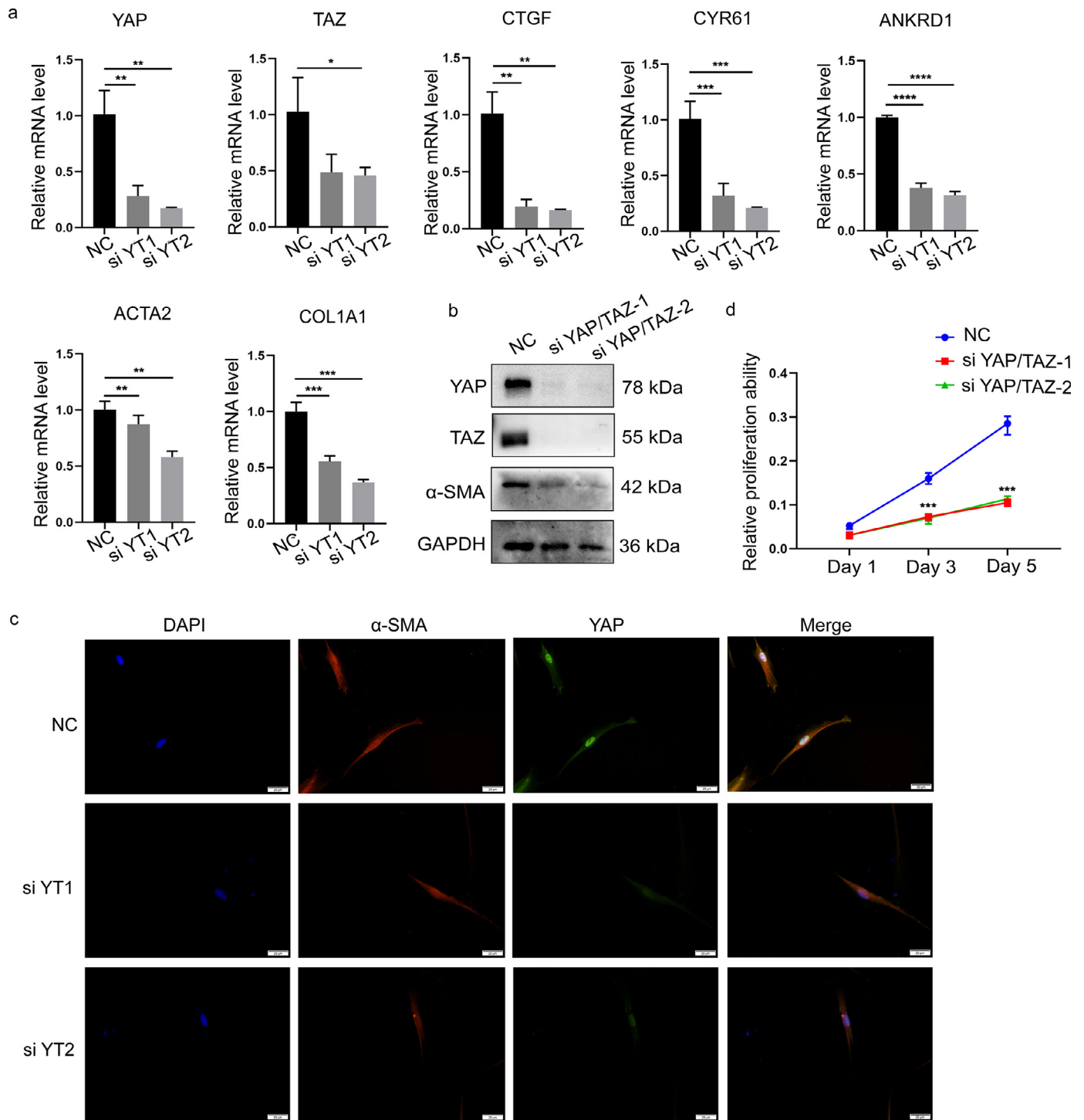
Figure 4. Knockdown of YAP/TAZ inhibits the expression of fibrotic genes and cell proliferation in intestinal fibroblasts. (a) The effect of YAP/TAZ knockdown on target genes and fibrotic genes in intestinal fibroblasts derived from stenotic regions of intestines from CD patients. (b) Western blot analysis was used to examine the effects of YAP/TAZ knockdown on α-SMA expression in fibroblasts isolated from stenotic intestine from CD patients. (c) Representative images of immunofluorescence staining showing the effect of intestinal fibroblasts with YAP/TAZ knockdown on α-SMA. Scale bar = 20 μm. (d) Knocking down YAP/TAZ expression changed the proliferation of CD fibroblasts, as determined by a CCK-8 assay. Statistical analyses were performed using Student's t test. Statistical differences are shown by *p<0.05, **p<0.01, ***p<0.001, and ****p<0.0001. All data shown are from three independent experiments.

expression had lower intestinal obstruction-free survival (p=0.0204) than those with low ROCK1 expression (Figure 7c). Additionally, the expression of ROCK1 was positively correlated with YAP/TAZ expression (R=0•4714, p=0•0019; R=0.4496, p=0•0032) (Figure 7d-e). Taken together, these data suggest that increased ROCK1 expression in obstructed tissues is significantly associated with YAP/TAZ expression and indicates worse clinical outcomes in CD.

Discussion

In this study, we discovered that YAP/TAZ, transcriptional effectors of the Hippo pathway, modulated the activation of intestinal fibroblasts. Increased YAP/TAZ levels play a profibrotic role in intestinal fibroblasts, which is associated with worse intestinal obstruction-free survival in CD patients. We also revealed that the antifibrotic effect of a ROCK
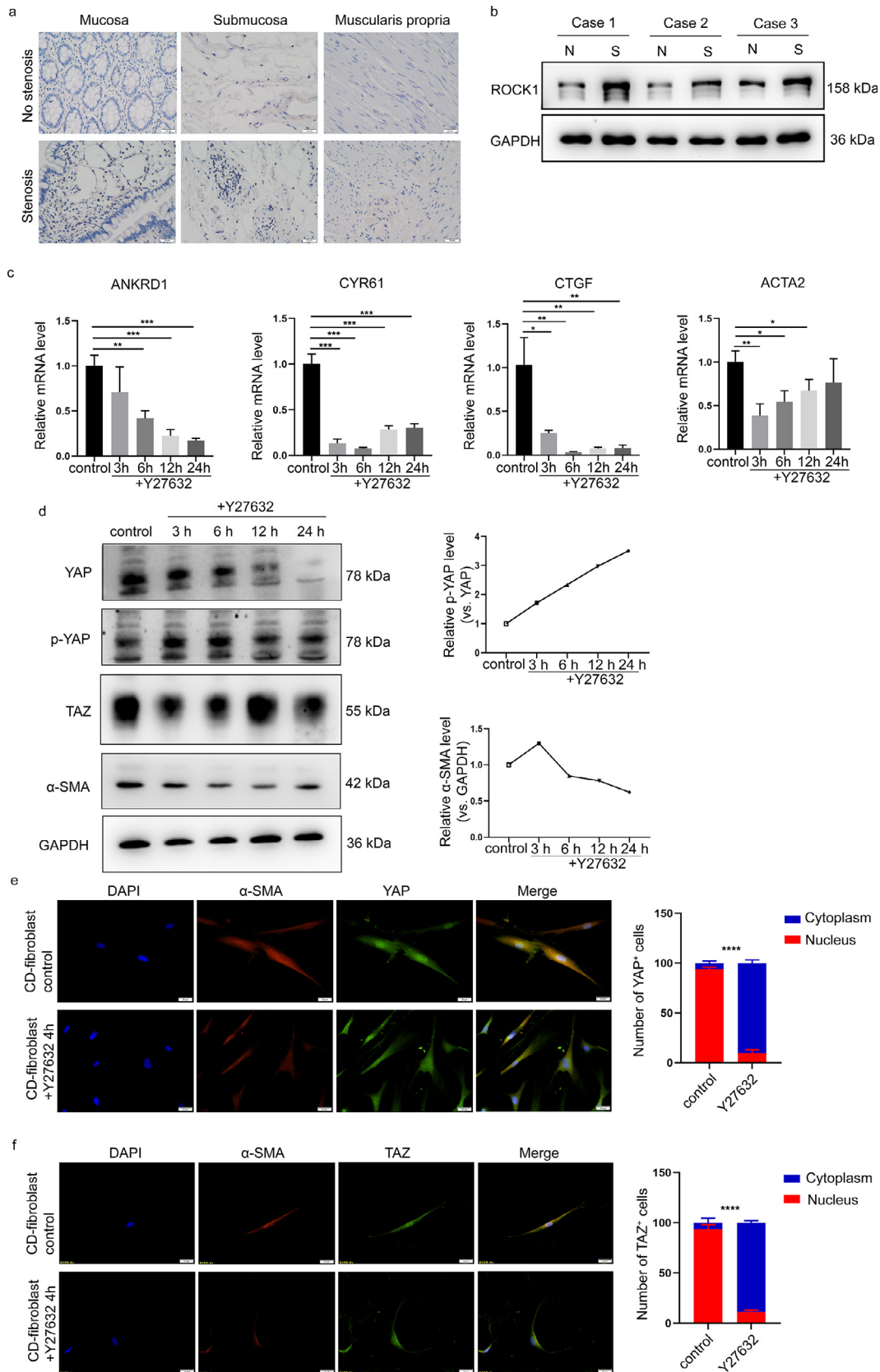
Figure 5. ROCK inhibition interferes with YAP/TAZ in intestinal fibroblasts. (a) Representative images of immunohistochemical staining showing the expression of ROCK1 in different layers of stenotic and nonstenotic intestinal tissue from CD patients (n=10). (b) Western blot analysis of ROCK1 expression in three paired samples of fibroblasts derived from CD patients with and without stenosis. (c) The effects of the ROCK inhibitor Y27632 on the target genes of YAP/TAZ and α-SMA in intestinal fibroblasts isolated from stenotic regions of the intestine. (d) The effect of the ROCK inhibitor Y27632 on YAP/TAZ expression, YAP phosphorylation and α-SMA expression was time dependent. (e-f) Representative images of immunofluorescence staining showing the effect of the ROCK inhibitor on YAP and TAZ localization. Scale bar = 20 μm. In all cases, the bars in the graphs represent the mean ± S.D. Statistical analyses were performed using Student's t test and a chi-square test. Significant differences are shown by **p<0.01, ***p<0.001, and ****p<0.0001. All data shown are from three independent experiments.

Figure 6. ROCK1 inhibitor reverses intestinal fibrosis in a chronic colitis murine model. (a) Schematic diagram of ROCK inhibitor treatment in a DSS-induced chronic colitis model. Mice were treated with 2% DSS to induce chronic inflammation and in the last cycle were intraperitoneally injected with vehicle or ROCK1 inhibitor. (b) Colorectal length, representative images of (c) haematoxylin−eosin-stained sections and (d) Masson's trichrome-stained sections and pathological scores of the distal colon in differently treated mice as described above (n=4 in each group). Scale bar = 100 μm. (e-f) Representative immunohistochemical images showing YAP/TAZ expression examined using an anti-YAP antibody and anti-TAZ antibody in colonic tissues from mice in different groups. Scale bar =50 μm (upper panels) and 20 μm (lower panels). (g-i) Representative immunofluorescence images of α-SMA, fibronectin/FN1 and collagen I expression in colonic tissues from mice in different groups. Scale bar =20 μm. In all cases, the bars in the graphs represent the mean ± S.D. Statistical analyses were performed using Student's t test for continuous variables and Mann-Whitney test for histological scores. Significant differences are shown by *p<0.05, **p<0.01, and ***p<0.001.

inhibitor on intestinal fibrosis was associated with inhibition of YAP/TAZ. Thus, our data suggest that YAP/TAZ is crucial in the pathogenesis of CD intestinal fibrosis and may serve as a potential therapeutic target for antifibrotic intervention in clinical practice.

The mechanism of intestinal fibroblast activation has not been fully elucidated. Thus, it is considerably imperative for clinicians to understand intestinal fibroblast activation to develop better treatment for CD patients. Numerous studies of human fibrotic diseases have revealed that YAP/TAZ is a key regulator involved in fibroblast activation and matrix formation. YAP/TAZ activity reflects the capacity for cell adhesion and response to mechanical stimulation.[36] Compared with fibroblasts in the stationary state, YAP/TAZ expression is higher in activated fibroblasts and shows significant nuclear accumulation in lung fibrosis and pancreatic cancer.[36,37] Consistent with the findings in other fibrotic diseases, our study demonstrated YAP/TAZ activation and enhanced YAP/TAZ-induced profibrotic gene expression in intestinal fibroblasts in CD, which indicates that YAP/TAZ is a promising general drug target for fibrotic diseases.

The effects of YAP/TAZ on fibroblast activation include promoting cell proliferation, increasing α-SMA expression and regulating ECM formation and degradation. YAP/TAZ can act in coordination with the TGF-β signalling pathway to promote the production of profibrotic factors (CTGF and PAI-1) and ECM-related genes. In addition to activating profibrotic gene expression, the effect of YAP/TAZ on promoting fibroblast proliferation also plays a vital role in fibroblast activation by expanding the cell pool of profibrotic fibroblasts. YAP/TAZ is well known as a key player regulating organ size, and activation of YAP/TAZ promotes cell proliferation in multiple solid cancers by activating the expression of cell cycle-related and antiapoptotic genes, mainly through TEAD transcription factors.[38] Similar regulatory mechanisms may exist in fibroblasts and need to be explored by gene expression profiling in future studies. Moreover, we found that inhibition of YAP/TAZ in fibroblasts decreased α-SMA expression, although the mechanism was not elucidated in this study. Previous evidences has demonstrated that YAP/TAZ can form a complex with SMAD protein in brain colloid cells, promoting the activation of
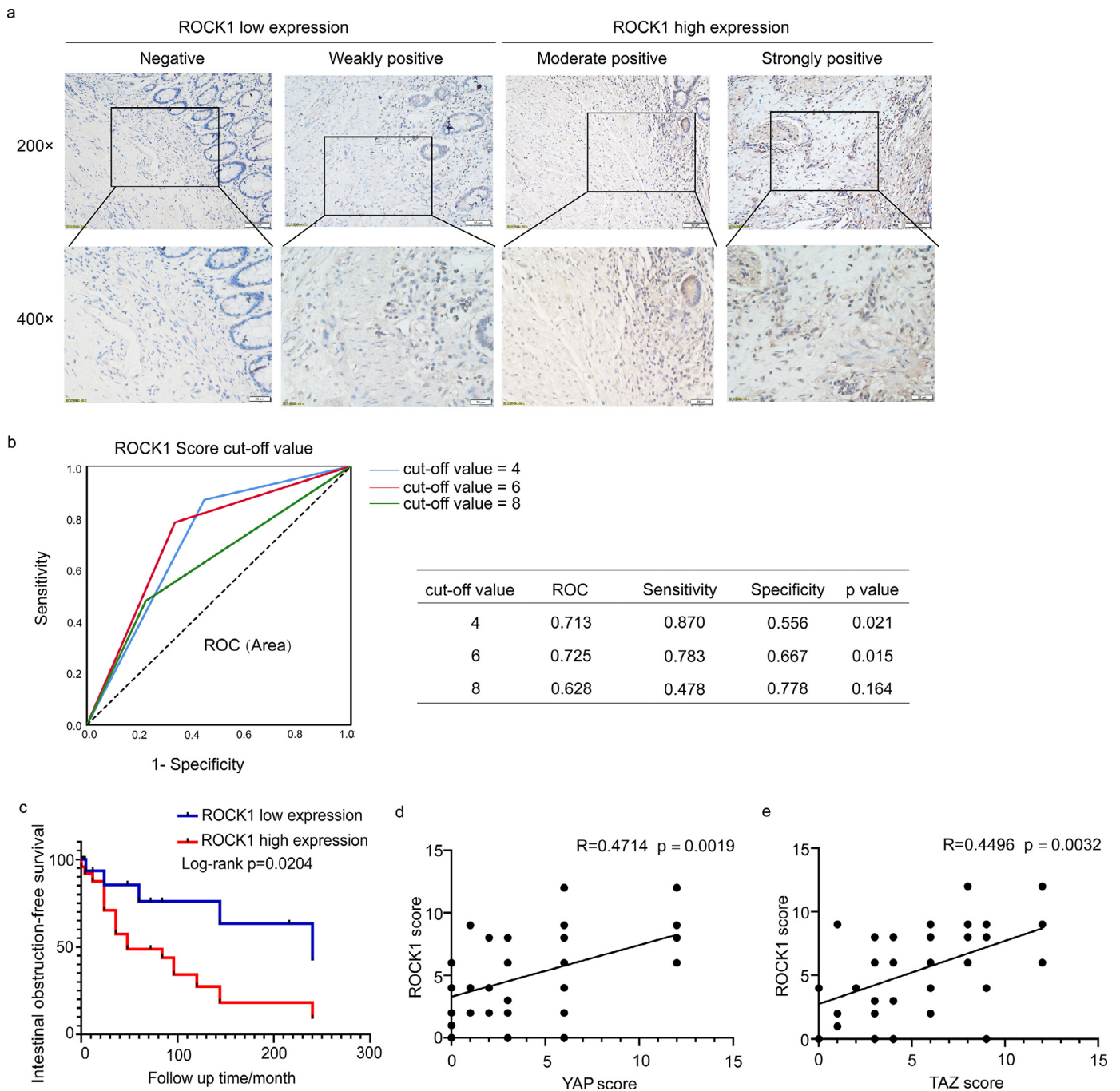
Figure 7. ROCK1 expression is increased in CD with intestinal obstruction and correlated with YAP/TAZ expression. (a) Immunohistochemical analysis of ROCK1 expression in CD patients. Scale bar = 50 μm (upper panels) and 20 μm (lower panels). (b) Cut-off value of the ROCK1 expression score in IHC analysis based on the ROC curve. The sensitivity and specificity of the selected cut-off value are shown in the table near the ROC curve. (c) Kaplan-Meier plots were stratified by ROCK1 expression for intestinal obstruction-free survival in CD patients. (d-e) The ROCK1 score was correlated with the YAP/TAZ score in CD patients. The ROC curve was used to determine the cut-off value. A log-rank test was performed for prognosis analysis. Spearman's correlation was used for correlation of rank data. Significant differences are shown by p = <0.05.

both.[39-41] In addition, previous studies have confirmed that SMAD3 can directly bind to α-SMA promoter regions.[42] Therefore, we infer that the YAP/TAZ-mediated Hippo pathway might promote α-SMA by regulating SMAD3 activation, which could be explored in the future.

YAP/TAZ regulation of fibroblast activation is a complex process. In kidney disease, the interaction between YAP/TAZ and ECM forms a positive feedback loop, which activates fibroblasts and leads to kidney fibrosis.[19] Extracellular environments, including matrix hardness, acid-base conditions, and cytokines, inhibit YAP/TAZ phosphorylation

and promote nuclear translocation through a series of signalling pathways, such as the FAK/Rho, Rho/ROCK, TGF-β/SMAD and Wnt signalling pathways.[6,12,23] Among the above signalling pathways activating YAP/TAZ, ROCK is considered to be a target candidate for fibrotic disease treatment. Previous studies have reported that ROCK inhibition prevents intestinal fibrosis by diminishing MRTF and increasing autophagy in fibroblasts.[20,22] It has also been reported that YAP activity is regulated by Rho-ROCK signalling.[23,43] Inhibition of ROCK leads to YAP phosphorylation and protein degradation. Our study showed that ROCK inhibition prevents activation of intestinal

fibroblasts, which is associated with loss of YAP/TAZ nuclear localization and decreased YAP/TAZ expression. Given the strong effect of YAP/TAZ on fibroblast activation, inhibition of YAP/TAZ might be one of the mechanisms by which a ROCK inhibitor exerts its antifibrotic effect in CD.

Based on the vital role of YAP/TAZ in fibroblasts, YAP/TAZ are promising drug targets for fibrotic diseases. However, caution should be taken in the use of ROCK or YAP/TAZ inhibitors in the clinic. On the one hand, systemic medication causes many side effects, such as arterial hypotension.[44] Once these drugs act on the circulatory system, the medication must be administered carefully, although certain ROCK inhibitors have been developed to target the intestine.[22] On the other hand, YAP/TAZ and ROCK are expressed in a variety of cells in the intestine and play a crucial role in regulating multiple biological processes.[13] For example, the function of YAP/TAZ is required for LGR5+ intestinal stem cells to maintain intestinal homeostasis and plays a vital role in newly discovered revival stem cells, which contribute to intestinal regeneration after tissue injury.[11,45,46] Although verteporfin, a YAP/TAZ inhibitor, can not only inhibit differentiation from hepatic stellate cells to fibroblasts[16] but can also deactivate primary fibroblasts in Dupuytren's contracture,[47] we unexpectedly found that verteporfin enhances aggressive colitis in the experimental colitis mouse model, which may be due to inhibition of intestinal stem cells, as indicated by decreased Lgr5 expression (Supplementary Figure 5). Therefore, specifically targeting YAP/TAZ in intestinal fibroblasts may be an effective therapeutic strategy with weak side effects for treatment of intestinal obstruction in CD. A dopamine receptor D1 (DRD1) agonist has been shown to reverse lung and liver fibrosis through selective YAP/TAZ inhibition.[17] However, DRD1 is not expressed in intestinal fibroblasts based on our preliminary study (data not shown). Future studies should be conducted to achieve selective YAP/TAZ inhibition in intestinal fibroblasts.

The limitations of this study mainly included its retrospective nature and the relatively small CD patient sample size from a single centre, which cannot be representative of the wider population. For statistical analysis of risk factors for intestinal obstruction in CD, we first used a chi-square test and Fisher's exact test for univariate analysis to identify factors with significant differences. In the multiple logistic regression model, YAP and ROCK1 expression was associated with intestinal obstruction in CD, while there was no significant difference in TAZ expression. Because of the correlation between YAP and TAZ, we speculate that the small sample size led to this statistical result. Further multicentre studies with a larger cohort should be conducted to investigate whether YAP is an independent risk factor for intestinal obstruction in CD.

YAP/TAZ are significantly increased in the stenotic intestines of CD patients and in an experimental chronic colitis murine model. Additionally, YAP/TAZ are required for the activation of intestinal fibroblasts, whose high expression is associated with intestinal obstruction in CD. The effect of the ROCK inhibitor on alleviating intestinal fibrosis was associated with inhibition of YAP/TAZ in fibroblasts. Thus, selective inhibition of YAP/TAZ in fibroblasts may be a promising therapeutic strategy for intestinal fibrosis in CD.

Contributors

Peng Du and Chen-Ying Liu conceived the research. Weijun Ou conducted the experiments, analysed all data, and wrote the manuscript. Weimin Xu and Fangyuan Liu assisted to design and perform the mice experiments and revised the manuscript. Weijun Ou, Weimin Xu and Fangyuan Liu verified the underlying data. Yuegui Guo and Zhenyu Huang collaborated to collected intestinal biopsies of CD patients and intestinal fibroblasts isolation. Tienan Feng provided guidance on the statistics of this study. All authors read and approved the final version of the manuscript.

Data sharing

All data supporting the conclusions of this study are included within the article and its additional file. RNA-sequence data generated in this manuscript are available at NCBI's Gene Expression Omnibus and publicly accessible through GEO Series accession number GSE174460.

Declaration of Competing Interest

All authors have nothing to disclose.

Acknowledgements

Supplementary materials

Supplementary material associated with this article can be found, in the online version, at doi:10.1016/j.ebiom.2021.103452.

References

1 Burke JP, Mulsow JJ, O'Keane C, Docherty NG, Watson RW, O'Connell PR. Fibrogenesis in Crohn's disease. Am J Gastroenterol 2007;102:439–48.

2 Thia KT, Sandborn WJ, Harmsen WS, Zinsmeister AR, Loftus EV. Risk factors associated with progression to intestinal complications of Crohn's disease in a population-based cohort. Gastroenterology 2010;139:1147–55.

3 Rieder F, Zimmermann EM, Remzi FH, Sandborn WJ. Crohn's disease complicated by strictures: a systematic review. Gut 2013;62:1072–84.

4 Gordon IO, Bettenworth D, Bokemeyer A, et al. Histopathology scoring systems of stenosis associated with small bowel crohn's disease: a systematic review. Gastroenterology 2020;158:137–50 e1.

5 Rieder F, Fiocchi C. Intestinal fibrosis in IBD−a dynamic, multifactorial process. Nat Rev Gastroenterol Hepatol 2009;6:228–35.

6 Piersma B, Bank RA, Boersema M. Signaling in fibrosis: TGF-beta, WNT, and YAP/TAZ converge. Front Med (Lausanne) 2015;2:59.

7 Olive KP, Jacobetz MA, Davidson CJ, et al. Inhibition of Hedgehog signaling enhances delivery of chemotherapy in a mouse model of pancreatic cancer. Science 2009;324:1457–61.

8 Laurenson S, Sidhu R, Goodall M, Adler AI. NICE guidance on nintedanib for treating idiopathic pulmonary fibrosis. Lancet Respir Med 2016;4:176–7.

9 Raghu G, Collard HR, Egan JJ, et al. An official ATS/ERS/JRS/ALAT statement: idiopathic pulmonary fibrosis: evidence-based guidelines for diagnosis and management. Am J Respir Crit Care Med 2011;183:788–824.

10 Rieder F, Fiocchi C. Mechanisms of tissue remodeling in inflammatory bowel disease. Dig Dis 2013;31:186–93.

11 Moya IM, Halder G. Hippo-YAP/TAZ signalling in organ regeneration and regenerative medicine. Nat Rev Mol Cell Biol 2019;20:211–26.

12 Totaro A, Panciera T, Piccolo S. YAP/TAZ upstream signals and downstream responses. Nat Cell Biol 2018;20:888–99.

13 Panciera T, Azzolin L, Cordenonsi M, Piccolo S. Mechanobiology of YAP and TAZ in physiology and disease. Nat Rev Mol Cell Biol 2017;18:758–70.

14 Qin Z, Xia W, Fisher GJ, Voorhees JJ, Quan T. YAP/TAZ regulates TGF-beta/Smad3 signaling by induction of Smad7 via AP-1 in human skin dermal fibroblasts. Cell Commun Signal 2018;16:18.

15 Alsamman S, Christenson SA, Yu A, et al. Targeting acid ceramidase inhibits YAP/TAZ signaling to reduce fibrosis in mice. Sci Transl Med 2020;12:eaay8798.

16 Mannaerts I, Leite SB, Verhulst S, et al. The Hippo pathway effector YAP controls mouse hepatic stellate cell activation. J Hepatol 2015;63:679–88.

17 Haak AJ, Kostallari E, Sicard D, et al. Selective YAP/TAZ inhibition in fibroblasts via dopamine receptor D1 agonism reverses fibrosis. Sci Transl Med 2019;11: eaau6296.

18 Martin K, Pritchett J, Llewellyn J, et al. PAK proteins and YAP-1 signalling downstream of integrin beta-1 in myofibroblasts promote liver fibrosis. Nat Commun 2016;7:12502.

19 Liang M, Yu M, Xia R, et al. Yap/Taz deletion in Gli(+) cell-derived myofibroblasts attenuates fibrosis. J Am Soc Nephrol 2017;28:3278–90.

20 Feng Y, LoGrasso PV, Defert O, Li R. Rho kinase (ROCK) inhibitors and their therapeutic potential. J Med Chem 2016;59:2269–300.

21 Yu B, Sladojevic N, Blair JE, Liao JK. Targeting Rho-associated coiled-coil forming protein kinase (ROCK) in cardiovascular fibrosis and stiffening. Expert Opin Ther Targets 2020;24:47–62.

22 Holvoet T, Devriese S, Castermans K, et al. Treatment of intestinal fibrosis in experimental inflammatory bowel disease by the pleiotropic actions of a local rho kinase inhibitor. Gastroenterology 2017;153:1054–67.

23 Dupont S, Morsut L, Aragona M, et al. Role of YAP/TAZ in mechanotransduction. Nature 2011;474:179–83.

24 Satsangi J, Silverberg MS, Vermeire S, Colombel JF. The Montreal classification of inflammatory bowel disease: controversies, consensus, and implications. Gut 2006;55:749–53.

25 Xu W, Ou W, Guo Y, et al. Clinical outcomes and risk factors of secondary extraintestinal manifestation in ulcerative colitis: results of a multicenter and long-term follow-up retrospective study. PeerJ 2019;7:e7194.

26 Neufert C, Becker C, Tureci O, et al. Tumor fibroblast-derived epiregulin promotes growth of colitis-associated neoplasms through ERK. J Clin Invest 2013;123:1428–43.

27 Xu W, Guo Y, Huang Z, et al. Small heat shock protein CRYAB inhibits intestinal mucosal inflammatory responses and protects barrier integrity through suppressing IKKβ activity. Mucosal immunology 2019;12:1291–303.

28 Liu F, Ou W, Tang W, et al. Increased AOC1 Expression Promotes Cancer Progression in Colorectal Cancer. Front Oncol 2021;11:657210.

29 Wirtz S, Popp V, Kindermann M, et al. Chemically induced mouse models of acute and chronic intestinal inflammation. Nat Protoc 2017;12:1295–309.

30 Yu B, Sladojevic N, Blair JE, Liao JK. Targeting Rho-associated coiled-coil forming protein kinase (ROCK) in cardiovascular fibrosis and stiffening. Expert Opin Ther Targets 2020;24:47–62.

31 Wirtz S, Popp V, Kindermann M, et al. Chemically induced mouse models of acute and chronic intestinal inflammation. Nat Protoc 2017;12:1295–309.

32 Zappa M, Stefanescu C, Cazals-Hatem D, et al. Which magnetic resonance imaging findings accurately evaluate inflammation in small bowel Crohn's disease? A retrospective comparison with surgical pathologic analysis. Inflamm Bowel Dis 2011;17:984–93.

33 Theiss AL, Fuller CR, Simmons JG, Liu B, Sartor RB, Lund PK. Growth hormone reduces the severity of fibrosis associated with chronic intestinal inflammation. Gastroenterology 2005;129:204–19.

34 Remmele W, Stegner HE. Recommendation for uniform definition of an immunoreactive score (IRS) for immunohistochemical estrogen receptor detection (ER-ICA) in breast cancer tissue. Pathologe 1987;8:138–40.

35 Zhao B, Li L, Tumaneng K, Wang CY, Guan KL. A coordinated phosphorylation by Lats and CK1 regulates YAP stability through SCF(beta-TRCP). Genes Dev 2010;24:72–85.

36 Liu F, Lagares D, Choi KM, et al. Mechanosignaling through YAP and TAZ drives fibroblast activation and fibrosis. Am J Physiol Lung Cell Mol Physiol 2015;308:L344–57.

37 Morvaridi S, Dhall D, Greene MI, Pandol SJ, Wang Q. Role of YAP and TAZ in pancreatic ductal adenocarcinoma and in stellate cells associated with cancer and chronic pancreatitis. Sci Rep 2015;5:16759.

38 Zhu C, Li L, Zhao B. The regulation and function of YAP transcription co-activator. Acta Biochim Biophys Sin (Shanghai) 2015;47:16–28.

39 Pefani DE, Pankova D, Abraham AG, et al. TGF-beta targets the hippo pathway scaffold RASSF1A to Facilitate YAP/SMAD2 nuclear translocation. Mol Cell 2016;63:156–66.

40 Huang Z, Hu J, Pan J, et al. YAP stabilizes SMAD1 and promotes BMP2-induced neocortical astrocytic differentiation. Development 2016;143:2398–409.

41 Nallet-Staub F, Yin X, Gilbert C, et al. Cell density sensing alters TGF-beta signaling in a cell-type-specific manner, independent from Hippo pathway activation. Dev Cell 2015;32:640–51.

42 Hu B, Wu Z, Phan SH. Smad3 mediates transforming growth factor-beta-induced alpha-smooth muscle actin expression. Am J Respir Cell Mol Biol 2003;29:397–404.

43 Kang PH, Schaffer DV, Kumar S. Angiomotin links ROCK and YAP signaling in mechanosensitive differentiation of neural stem cells. Mol Biol Cell 2020;31:386–96.

44 Olson MF. Applications for ROCK kinase inhibition. Curr Opin Cell Biol 2008;20:242–8.

45 Yui S, Azzolin L, Maimets M, et al. YAP/TAZ-dependent reprogramming of colonic epithelium links ECM remodeling to tissue regeneration. Cell Stem Cell 2018;22:35–49 e7.

46 Ayyaz A, Kumar S, Sangiorgi B, et al. Single-cell transcriptomes of the regenerating intestine reveal a revival stem cell. Nature 2019;569:121–5.

47 Piersma B, de Rond S, Werker PM, et al. YAP1 is a driver of myofibroblast differentiation in normal and diseased fibroblasts. Am J Pathol 2015;185:3326–37.